Received: 21 June 2021 | Revised: 24 July 2021 | Accepted: 27 July 2021

DOI: 10.1002/jmv.27244

RESEARCH ARTICLE

JOURNAL OF MEDICAL VIROLOGY WILEY

SARS-CoV-2 pseudovirus infectivity and expression of viral entry-related factors ACE2, TMPRSS2, Kim-1, and NRP-1 in human cells from the respiratory, urinary, digestive, reproductive, and immune systems

Fei Zhang[1,2] | Wan Li[1,2] | Jian Feng[1,2] | Suzane Ramos da Silva[1,2] | Enguo Ju[1,2] | Hu Zhang[1,2] | Yuan Chang[1,2] | Patrick S. Moore[1,2] | Haitao Guo[1,2] | Shou-Jiang Gao[1,2]

[1]Cancer Virology Program, UPMC Hillman Cancer Center, University of Pittsburgh School of Medicine, Pittsburgh, Pennsylvania, USA

[2]Department of Microbiology and Molecular Genetics, University of Pittsburgh School of Medicine, Pittsburgh, Pennsylvania, USA

Correspondence

Shou-Jiang Gao, PhD, Cancer Virology Program, UPMC Hillman Cancer Center, University of Pittsburgh School of Medicine, Pittsburgh, PA 15213, USA.
Email: gaos8@upmc.edu

Funding information

UPMC Hillman Cancer Center Startup Fund; Pittsburgh Foundation Endowed Chair in Drug Development for Immunotherapy

Abstract

Infection by severe acute respiratory syndrome coronavirus 2 (SARS-CoV-2) causes a wide spectrum of syndromes involving multiple organ systems and is primarily mediated by viral spike (S) glycoprotein through the receptor-binding domain (RBD) and numerous cellular proteins including ACE2, transmembrane serine protease 2 (TMPRSS2), kidney injury molecule-1 (Kim-1), and neuropilin-1 (NRP-1). In this study, we examined the entry tropism of SARS-CoV-2 and SARS-CoV using S protein-based pseudoviruses to infect 22 cell lines and 3 types of primary cells isolated from respiratory, urinary, digestive, reproductive, and immune systems. At least one cell line or type of primary cell from each organ system was infected by both pseudoviruses. Infection by pseudoviruses is effectively blocked by S1, RBD, and ACE2 recombinant proteins, and more weakly by Kim-1 and NRP-1 recombinant proteins. Furthermore, cells with robust SARS-CoV-2 pseudovirus infection had strong expression of either ACE2 or Kim-1 and NRP-1 proteins. ACE2 glycosylation appeared to be critical for the infections of both viruses as there was a positive correlation between infectivity of either SARS-CoV-2 or SARS-CoV pseudovirus with the level of glycosylated ACE2 (gly-ACE2). These results reveal that SARS-CoV-2 cell entry could be mediated by either an ACE2-dependent or -independent mechanism, thus providing a likely molecular basis for its broad tropism for a wide variety of cell types.

KEYWORDS

Angiotensin-converting enzyme 2 (ACE2), and glycosylation, Kim-1, NRP-1, pseudovirus, receptor binding domain (RBD), SARS-CoV, SARS-CoV-2, spike protein, TMPRSS2, viral entry tropism, virus receptor

1 | INTRODUCTION

During the coronavirus disease 2019 (COVID-19) pandemic, severe acute respiratory syndrome coronavirus 2 (SARS-CoV-2) infection has manifested high transmission efficiency and complex clinical features affecting multiple human organ systems.[1,2] Apart from the respiratory system, increasing evidence shows that SARS-CoV-2 infects urinary, digestive, reproductive, neurological, and immune system organs, causing a wide range of clinical symptoms such as dry cough, diarrhea, acute kidney injury, neurological complications, and various degrees of liver damage.[3] Indeed, RNA-sequencing (RNAseq), reverse-transcription PCR (RT-PCR), and immunohistochemistry (IHC) have shown SARS-CoV-2 to be present

TABLE 1 Cell lines used in the present study

Cell name	Origin	Source of cell	Culture medium
Respiratory system			
JHU-029	Laryngeal squamous cell carcinoma	CVCL_5993	RPMI-1640 complete medium
NCL H460	Large cell lung cancer	ATCC HTB-177	RPMI-1640 complete medium
NCL H322	Large cell lung cancer	ATCC CRL5806	DMEM complete medium
NCL H520	Large cell lung cancer	ATCC HTB-182	DMEM complete medium
A549	Lung adenocarcinoma	ATCC CRM-CCL-185	DMEM complete medium
Primary human lobar bronchial epithelial cells (HLBEC)	Lobar bronchial tissue	Lifeline® Cell Technology	Lifeline® BronchiaLife™ Medium
Primary human small airway epithelial cells (HSAEC)	Small airway tissue	Lifeline® Cell Technology	Lifeline® BronchiaLife™ Medium
Urinary system			
769-P	Renal cell adenocarcinoma	ATCC CRL-1933	RPMI-1640 complete medium
768-O	Renal cell adenocarcinoma	ATCC CRL-1932	RPMI-1640 complete medium
A498	Renal cell adenocarcinoma	ATCC HTB-44	RPMI-1640 complete medium
Caki-1	Renal cell carcinoma	ATCC HTB-46	DMEM complete medium
ACHN	Renal cell adenocarcinoma	ATCC CRL-1611	DMEM complete medium
HRC45	Renal cell carcinoma	CVCL_IS24	DMEM complete medium
HRC63	Renal cell carcinoma	CVCL_IS25	DMEM complete medium
HRC59	Renal cell carcinoma	FCCC	DMEM complete medium
Immune system			
BCP-1	Primary effusion lymphoma	ATCC CRL-2294	RPMI-1640 complete medium
BC-3	Primary effusion lymphoma	ATCC CRL-2277	RPMI-1640 complete medium
BJAB	Primary effusion lymphoma	CVCL_5711	RPMI-1640 complete medium
THP-1	Acute monocytic leukemia	ATCC TIB-202	RPMI-1640 complete medium
Digestive system			
Huh-7	Hepatocellular carcinoma cell	JCRB0403	DMEM complete medium
PCI-13	Oral cavity squamous cell carcinoma	CVCL_C182	RPMI-1640 complete medium
UD-SCC-2	Hypopharyngeal squamous cell carcinoma	CVCL_E325	RPMI-1640 complete medium
Reproductive system			
HUVEC	Umbilical Vein Endothelial Cells	ATCC PCS-100-010	ECBM(Cell applications, 210-490)
T47D	Ductal carcinoma	ATCC HTB-133	RPMI-1640 complete medium
MCF-7	Breast adenocarcinoma	ATCC HTB-22	RPMI-1640 complete medium

Note: DMEM or RPMI-1640 complete medium is made of DMEM or RPMI-1640 basal medium with 10% fetal bovine serum (FBS) and 1% Penicillin-Streptomycin 100× Solution (25-512, GenClone).

Abbreviations: DMEM, Dulbecco's modified Eagle medium; HUVEC, human umbilical vein endothelial cells.

in cells from different organ systems during natural infection. Besides lung and kidney cells,[4,5] SARS-CoV-2 RNA or proteins have been detected in the liver,[6] placenta,[7] intestine,[8] and immune cells.[9] In lung tissues from severe COVID-19 patients, SARS-CoV-2 infection has been detected in an extensive range of parenchymal cells including type II pneumocytes, ciliated, goblet, club-like, and endothelial cells (ECs) as well as immune cells including macrophages, monocytes, neutrophils, and natural killer (NK), B and T cells with up to 90% of them positive for viral proteins, providing additional evidence for a broad SARS-CoV-2 cell tropism.[10] The numbers of cells infected are associated with the extent of tissue damage,

TABLE 2 Primers used in this study

Gene	Primer	Sequence (5′–3′)
β-actin	β-actin-F	CCCTGGACTTCGAGCAAGAG
	β-actin-R	ACTCCATGCCCAGGAAGGAA
ACE2	qACE2-F	GGGATCAGAGATCGGAAGAAGAAA
	qACE2-R	AGGAGGTCTGAACATCATCAGTG
TMPRSS2	qTMPRSS2-F	AATCGGTGTGTTCGCCTCTAC
	qTMPRSS2-R	CGTAGTTCTCGTTCCAGTCGT
Kim-1	Kim-1-qPCR-F	GACAACGAGCATTCCAACAA
	Kim-1-qPCR-R	GCTGAGGTGAAGATGGTGAAG
NRP1	Nrp1-qPCR-F	CATCAATTTTAATTTCTGGGTTCTTT
	Nrp1-qPCR-R	CACATTTCACAAGAAGATTGTGC

Abbreviations: TMPRSS2, transmembrane serine protease 2; Kim-1, kidney injury molecule-1; NRP-1, neuropilin-1.

supporting a direct role of SARS-CoV-2 infection in causing the complex pathologies of COVID-19.[10]

The tropism of SARS-CoV-2 infection for various cell types is key to understanding these pathologic and clinical COVID-19 features. Numerous cell lines are permissive to SARS-CoV-2 infection in cell culture. Vero E6, an African green monkey kidney cell line, has been widely used in SARS-CoV-2 culture.[11,12] Several cell lines from the digestive system (Caco-2) and liver system (Huh-7) are permissive to SARS-CoV-2 infection,[13] and Calu-3 cells isolated from the human respiratory system have been used in SARS-CoV-2 infection studies.[14–16] Interestingly, primary human alveolar epithelial cells (AECs) and the lung A549 cell line are refractory to infection by both SARS-CoV-2 and SARS-CoV.[13,17,18]

Numerous cellular proteins have been identified to mediate SARS-CoV-2 entry including angiotensin-converting enzyme 2 (ACE2),[19,20] transmembrane serine protease 2 (TMPRSS2),[21] kidney injury molecule-1 (Kim-1), a biomarker for human renal proximal tubule injury,[22,23] and neuropilin-1 (NRP-1), which binds to furin-cleaved substrates.[24,25] Single-cell RNAseq analysis has shown that ACE2 is expressed in lung type II pneumocytes (AT2 cells), liver cholangiocytes, colon colonocytes, esophagus keratinocytes, ileum ECs, rectum ECs, stomach epithelial cells, and kidney proximal tubule cells.[26] ACE2 protein also has been detected in enterocytes, renal tubule cells, gallbladder cells, cardiomyocytes, male reproductive cells, placental trophoblasts, ductal cells, and cells from eye tissues, and vasculature and respiratory systems.[27] Nasal epithelial cells, the initial site for virus entry and likely reservoir for dissemination between individuals, have high ACE2 and TMPRSS2[28] expression levels. Moreover, ACE2 and TMPRSS2 are expressed in a transient secretory cell type.[29] The expression of ACE2 and TMPRSS2 proteins in broad cell types suggests that they might play critical roles in SARS-CoV-2 infection and spread. In contrast, few studies so far have examined the expression and distribution of the alternative receptors Kim-1 and NRP-1 in different cells and tissues despite their implicated roles in SARS-CoV-2 entry. In lung tissues from severe COVID-19 cases, ACE2 expression has been observed in a broad range of parenchymal and immune cells in agreement with the detection of SARS-CoV-2 proteins in these cells.[10] Interestingly, ACE2-negative SARS-CoV-2-infected cells have been detected in infected tissues, suggesting the likely presence of an ACE2-independent infection pathway.[10]

In this study, we investigated the infectivity of SARS-CoV-2 and SARS-CoV pseudoviruses in 22 cell lines and 3 primary cell types from 5 human organ systems including respiratory, urinary, digestive, reproductive, and immune systems, and demonstrated that at least 1 cell line or cell type from each of these organ systems is permissive for both SARS-CoV-2 and SARS-CoV pseudoviruses. We showed the expression of ACE2, TMPRSS2, Kim-1, and NRP-1 in a broad range of cells from the five human organ systems, and that cells infected by SARS-CoV-2 pseudovirus either expressed ACE2 or Kim-1 and NRP-1 proteins. Finally, we found a high degree of correlation between glycosylated ACE2 (gly-ACE2) and SARS-CoV-2 pseudovirus infectivity suggesting that posttranslational modification of ACE2 is critical for SARS-CoV-2 patency.

2 | MATERIALS AND METHODS

2.1 | Cell lines and cell culture

Cell lines and primary cells, sources, the organs and tissues where they are isolated, and culture conditions are listed in Table 1. Cells were maintained in their respective medium with 10% heat-inactivated fetal bovine serum (FBS) and 1% Penicillin-Streptomycin 100× Solution (25-512, Genesee). HEK293T cells and HEK293 ACE2 stable cells (CVD19-200A-1, SBI System Biosciences) were cultured in Dulbecco's Modified Eagle Medium (DMEM) with 10% FBS and 1% Penicillin-Streptomycin 100× Solution. HEK293T cells were used for pseudovirus packaging while HEK293 ACE2 stable cells were used for titration of pseudoviruses.

2.2 | Pseudovirus packaging

The plasmid sets used for packaging of pseudoviruses included the reporter plasmid pNL4-3. Luci.R-.E-expressing the firefly gene (3418, AIDS Reagent Program, National Institute of Health), pcDNA3.1-SARS-CoV-2-S expressing the codon-optimized spike protein gene from Wuhan-Hu-1 strain SARS-CoV-2, kindly provided by Dr. Wei Cun,[30] and pcDNA3.1-SARS-CoV-S expressing the spike protein gene from BJ302 strain SARS-CoV. pcDNA3.1(+) was used to generate a control "naked pseudovirus." A pseudovirus generated with pMD2.G expressing vesicular stomatitis virus (VSV) G envelope protein (VSV-G) was used as an additional control. To generate a pseudovirus, HEK293T cells were cotransfected with pNL4-3. Luci.R.-E- and pcDNA3.1-SARS-CoV-2-S, pcDNA3.1-SARS-CoV-S, pMD2.G, or pcDNA3.1(+) using a jetOPTIMUS transfection reagent (117-15, Polyplus). The supernatant was harvested at 48 h

posttransfection, centrifuged at 3,000 rpm for 10 min, aliquoted, and stored at −80°C for later use.

2.3 | Infectivity assay and blocking assay

To investigate the susceptibility of various cells to pseudoviruses, cells were seeded at 10^4 cells per well in a 96-well plate 1 day before infection. The medium was removed, and 100 µl of supernatant containing SARS-CoV-2 or SARS-CoV pseudovirus was added to the cells and incubated overnight. The medium was changed with fresh medium and cells were incubated for another 48 h and analyzed for luciferase activity using the Luciferase Assay System (E1501, Promega). HEK293 ACE2 stable cells were used to titrate and normalize the viral titers of different viral preparations.

We used Huh-7 cells to examine the effects of different recombinant proteins on the infectivity of SARS-CoV-2 or SARS-CoV pseudovirus. Recombinant proteins used in this study included SARS-CoV-2 spike S1-hFc (40591-V02H, Sino biological), SARS-CoV-2 spike receptor-binding domain (RBD) RBD-mFc (40592-V05H1, Sino biological), human ACE2-His (10108-H08H, Sino biological), human KIM-1/TIM-1-His&Fc (11051-H16H, Sino biological), human neuropilin (NRP)-1-hFc (10011-H02H, Sino biological), and human Fc protein (hFc, AG100, Sigma). The supernatant containing the pseudovirus was mixed with an equal volume of a specified recombinant protein diluted in medium to achieve the specified concentration at 37°C for 1 h, and used for the infection assay.

2.4 | ACE2 protein deglycosylation

Protein lysates of Huh7 were prepared in NP40 Cell Lysis Buffer (FNN0021, Thermo Fisher Scientific) according to the manufacture's instructions. Deglycosylation was performed using PNGase F Glycan Cleavage Kit (A39245, Thermo Fisher Scientific). The deglycosylated and nondeglycosylated samples were analyzed by Western blotting.

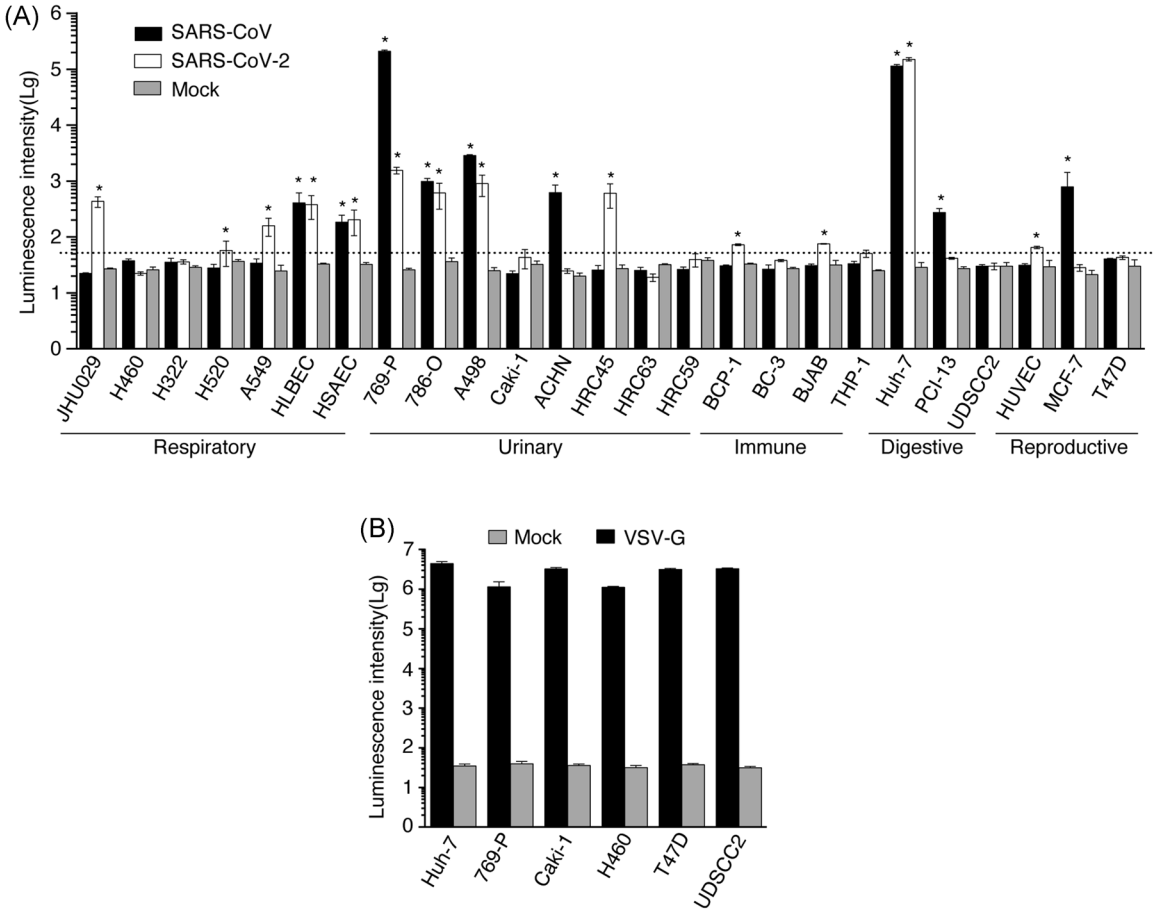

FIGURE 1 Infection of different types of cells from five human organ systems by SARS-CoV-2, SARS-CoV, and VSV-G pseudoviruses. (A) Infection of different types of cells from five human organ systems by SARS-CoV-2 and SARS-CoV pseudoviruses. An infection was considered positive and labeled with "*" when the luciferase signal was higher than the means of the uninfected cells (mock) plus 5 SEMs (dotted line). (B) Infection of different types of cells by VSV-G pseudovirus. SARS-CoV-2, severe acute respiratory syndrome coronavirus 2; SARS-CoV, severe acute respiratory syndrome coronavirus; VSV, vesicular stomatitis virus

TABLE 3 Tropism of SARS-CoV-2 and receptor distribution

Cell name	Luciferase activity			Relative expression levels									
				ACE2				TMPRSS2		Kim-1		NRP-1	
	SARS-CoV	SARS-CoV-2	Mock	Total	Gly	Un-gly	mRNA	Protein	mRNA	Protein	mRNA	Protein	mRNA
Respiratory system													
JHU029	22.33 ± 0.67	433.3 ± 93.54*	27.00 ± 1.16	8279	1131	7148	30.42	2087	26.92	3827	28.38	0	21.29
NCL H460	37.67 ± 2.85	22.33 ± 1.45	26.00 ± 3.06	5170	1246	3924	29.04	6720	28.49	2040	22.96	2996	20.19
NCL H322	35.33 ± 6.17	36.00 ± 3.22	28.67 ± 1.86	15387	9539	5848	23.42	2328	24.32	0	28.69	0	21.82
NCL H520	28.00 ± 4.58	57.33 ± 27.43*	37.00 ± 2.52	448	448	0	22.24	3987	21.92	0	23.05	0	19.85
A549	34.33 ± 6.12	160.0 ± 57.10*	24.67 ± 6.49	4601	271	4330	21.03	0	21.59	19544	15.30	16783	19.22
HLBEC	408.67 ± 208.99*	378.67 ± 172.20*	33.00 ± 1.16	13544	423	13121	25.50	0	28.50	0	28.72	879	19.88
HSAEC	185.33 ± 61.39*	204.33 ± 99.11*	32.67 ± 2.33	13724	624	13100	28.53	0	29.78	0	32.02	3011	19.75
Urinary system													
769-P	211471 ± 8974*	1555 ± 215.90*	26.00 ± 1.73	20436	14305	6131	20.30	1147	27.71	17436	15.45	7816	18.73
768-O	982.3 ± 131.4*	617.3 ± 304.00*	36.33 ± 5.93	11533	9520	2018	28.60	0	27.36	2622	18.40	11387	19.22
A498	2873 ± 110.90*	906.3 ± 374.10*	25.00 ± 3.46	20476	15492	4984	23.97	2768	27.32	19337	15.58	20782	17.40
Caki-1	22.00 ± 2.65	43.33 ± 16.37	32.67 ± 4.67	3146	888	2258	25.50	882	24.28	21953	15.51	13374	20.12
ACHN	622.3 ± 225.7*	24.67 ± 2.19	20.00 ± 2.65	5050	4905	145	26.80	16760	27.17	2903	16.83	16385	20.23
HRC-45	25.67 ± 5.24	607.7 ± 281.60*	27.33 ± 4.37	944	401	543	27.00	3951	25.83	15533	15.46	14228	20.13
HRC-63	25.33 ± 3.28	19.00 ± 2.89	32.00 ± 1.53	3812	571	3241	28.12	2340	27.31	9618	16.07	7017	19.36
HRC-59	26.33 ± 2.60	39.67 ± 10.73	38.00 ± 4.62	965	800	165	27.16	0	25.11	0	23.95	13139	18.35
Immune system													
BJAB	31.00±2.08	76.00±1.00*	31.67 ± 6.69	0	0	0	21.43	961	16.72	0	25.31	0	23.14
BCP-1	30.67±1.20	72.67±2.60*	33.00 ± 1.16	0	0	0	26.67	3627	21.73	0	28.89	4700	23.62
BC-3	26.67±4.98	38.00±1.73*	27.33 ± 1.33	0	0	0	26.06	0	25.78	0	31.17	0	29.15
THP-1	33.33±3.71*	51.00±7.51*	25.00 ± 1.16	1946	0	1946	32.67	2323	26.31	0	28.99	11857	22.68
Digestive system													
HuH-7	114797±7622*	151463±10774*	28.67 ± 6.17	12768	12045	723	19.52	0	24.47	11532	16.42	20991	20.77
PCI-13	276.3±47.35*	41.67±1.67*	27.33 ± 2.03	9431	4897	4534	22.02	0	22.64	0	32.26	0	21.66
UDSCC2	30.00±2.08	30.00±4.04	30.33 ± 4.63	8306	1069	7237	26.60	1930	26.92	2429	26.34	0	20.80

(Continues)

TABLE 3 (Continued)

Cell name	Luciferase activity			Relative expression levels									
				ACE2				TMPRSS2		Kim-1		NRP-1	
	SARS-CoV	SARS-CoV-2	Mock	Total	Gly	Un-gly	mRNA	Protein	mRNA	Protein	mRNA	Protein	mRNA
Reproductive system													
HUVEC	31.33±1.86	65.33±3.38	29.33 ± 8.88	7322	0	7322	28.04	0	31.32	0	31.69	25361	18.34
MCF-7	40.67±1.20	43.00±3.22	30.00 ± 9.07	1830	679	1151	25.90	631	22.67	1345	30.25	0	23.14
T47D	794.3±644.7*	28.33±3.76	21.33 ± 4.06	7040	2931	4109	23.05	13051	20.45	1256	27.60	0	24.47

Note: In the infection assay, luciferase activity higher than the mean of mock-infected cells plus 5 times of SEM was considered as "positive" and marked with "*."

Abbreviations: Kim-1, kidney injury molecule-1; mRNA, messenger RNA; NRP-1, neuropilin-1; SARS-CoV-2, severe acute respiratory syndrome coronavirus 2; SARS-CoV, severe acute respiratory syndrome coronavirus; TMPRSS2, transmembrane serine protease 2.

2.5 | Western blotting

Protein lysates were prepared in sample buffer and loaded onto a 12% sodium dodecyl sulfate–polyacrylamide gel electrophoresis (SDS-PAGE) gel. The proteins were transferred onto a nitrocellulose membrane (A13420267, GE Healthcare Life Science). The membranes were blocked with 5% nonfat milk at room temperature for 1 h and then incubated with primary antibodies diluted at 1:1000 in Tris-buffered saline with 0.1% Tween-20 (TBS-T) buffer containing 1% bovine serum albumin (BSA, Sigma) overnight at 4°C. The primary antibodies used were a rabbit polyclonal antibody to ACE2 (ab15348, Abcam), rabbit monoclonal antibodies to TMPRSS2 (EPR3861) (ab92323, Abcam), Kim-1 (E1R9N) (14971 S, CST) and NRP-1 (EPR3113) (ab81321, Abcam), and a mouse monoclonal antibody to β-tubulin. Following washing, the membranes were incubated with their respective secondary antibodies for 1 h at room temperature. Goat anti-rabbit horseradish peroxidase (HRP) conjugated IgG (7074 V, CST) and horse antimouse HRP conjugated antibody (7076 V, CST) were diluted at 1:5,000 in TBS-T with 1% BSA. After wash, the signal was detected with SuperSignal™ West Femto Maximum Sensitivity Substrate (34096, Thermo Fisher Scientific) and visualized with the ChemiDoc™ MP Imaging System (Bio-Rad). The intensity of the protein bands was quantified with the ImageJ Software.

2.6 | mRNA expression analysis

Reverse transcription-quantitative real-time PCR (RT-qPCR) was performed to analyze levels of transcripts. Briefly, total RNA was extracted using TRI Reagent (T9424-200ML, Sigma) according to the manufacturer's instructions. Total RNA was converted to complementary DNA (cDNA) using a High-Capacity cDNA Reverse Transcription Kit (4368814, Thermo Fisher Scientific). Quantitative real-time PCR (qPCR) was performed using SsoAdvanced™ Universal SYBR® Green Supermix (172-5272, Bio-Rad) in the CFX Connect Real-Time System (Bio-Rad). The specific primers were listed in Table 2. β-actin gene was used for normalization, and the relative expression levels were shown as C_t values.

2.7 | Immunofluorescence assay (IFA)

The expression levels and cellular localization of ACE2, Kim-1, and NRP-1 were analyzed by IFA in Huh-7, 769-P, HRC45, ACHN, H520, MCF-7, H322, HSAEC, and HLBEC cells. Cells seeded overnight on slides were treated with precooled methanol for 10 min at −20°C. Following incubation with primary antibodies of NRP-1, TMPRSS2, Kim-1, and ACE2 diluted at 1:200 in PBS with 3% BSA overnight at 4°C, and then a fluorescein isothiocyanate (FITC)-labeled secondary antibody for 1 h at room temperature,

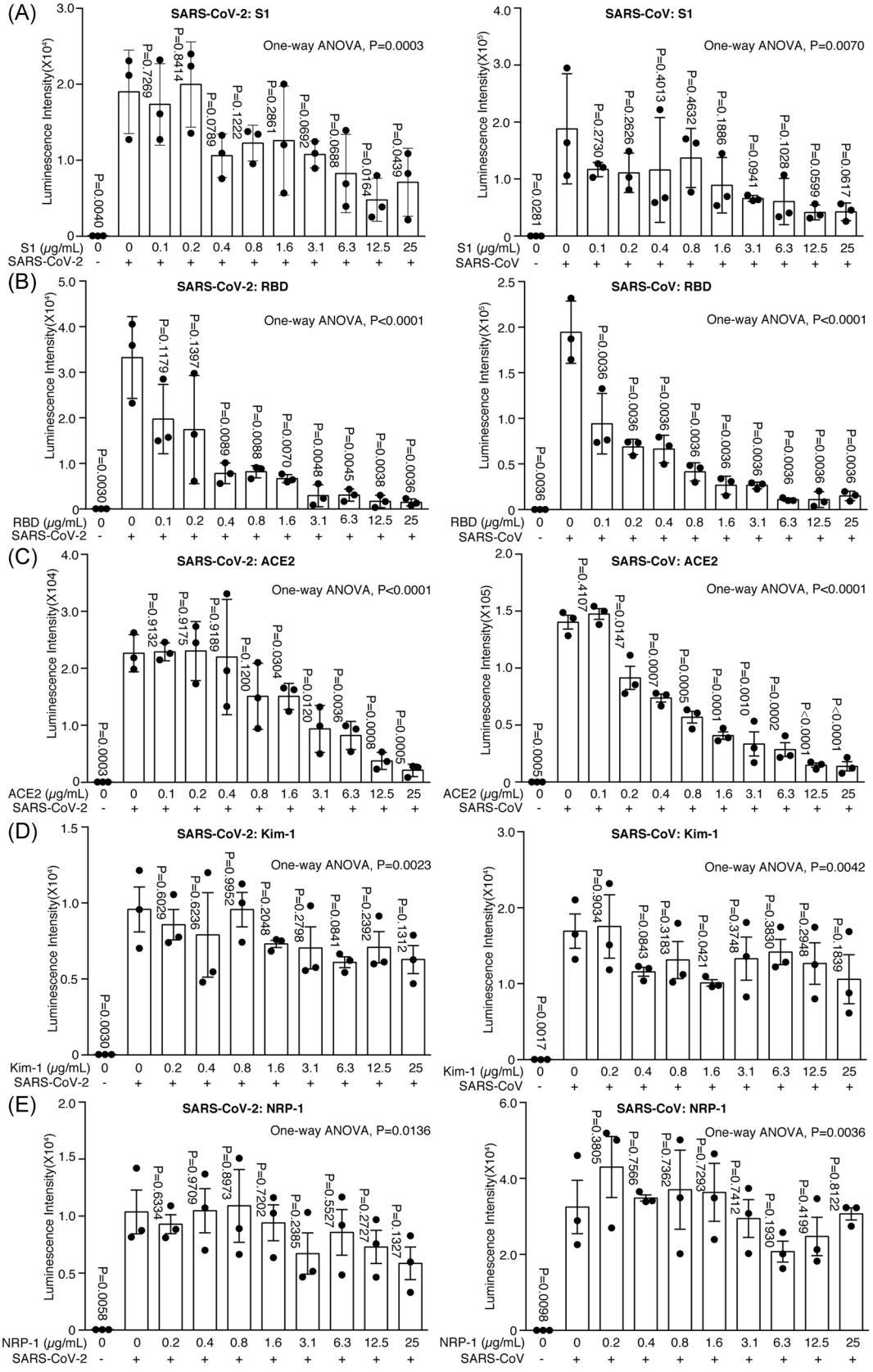

FIGURE 2 (See caption on next page)

the slides were stained with 4′,6-diamidino-2-phenylindole (DAPI) for 10 min at room temperature. The slides were sealed with MilliporeSigma™ Calbiochem™ FluorSave™ Reagent (345-578-920 ML, Thermo Fisher Scientific) and visualized with an Olympus IX83 Microscope.

2.8 | Statistical analysis

All the experiments were independently performed at least three times, each with at least three repeats. GraphPad Prism 6 was used for statistical analysis. Results were presented as mean ± standard error of the mean (SEM). One-way analysis of variance (ANOVA) was performed if multiple samples were involved. *p*-value was calculated by unpaired two-tailed Student's *t* test. $p < 0.05$ was considered statistically significant. Correlation analysis was performed by Pearson correlation analysis using Graphpad Prism 6, and the *p* and *r* values were presented.

3 | RESULTS

3.1 | SARS-CoV-2 pseudovirus can infect a wide range of cell types

To investigate the cell tropism, we used 22 cell lines and 3 types of primary cells isolated from five human organ systems for infection of SARS-CoV-2 and SARS-CoV pseudoviruses. Cells infected with pseudoviruses for 60 h were examined for luciferase activity. Cells infected with the "naked pseudovirus" were used as negative controls, which produced almost no luciferase signal similar to the mock-infected cells. We considered an infection as "positive" when the luciferase signal was higher than the mean of the mock-infected cells plus 5 SEMs (Figure 1A and Table 3). At least one cell line or cell type from each of the five organ systems gave positive signals after infection by SARS-CoV-2 pseudovirus. Strong signals were detected for both SARS-CoV-2 and SARS-CoV pseudoviruses in primary human lobar bronchial epithelial cells (HLBEC) and primary human small airway epithelial cells (HSAEC) from the respiratory system, 769-P, 786-O, and A498 cells from the urinary system, and Huh-7 cells from the digestive system.

Variations between SARS-CoV-2 and SARS-CoV pseudoviruses were observed for several cell lines. Strong signals were observed in JHU029 and A549 cells from the respiratory system, and HRC45 cells from the urinary system for SARS-CoV-2 but not SARS-CoV pseudovirus. In contrast, robust infection was observed for urinary ACHN cells, digestive system PCI-13 cells, and breast tumor MCF-7 cells for SARS-CoV but not SARS-CoV-2 pseudovirus. Weak but significant pseudovirus infections were also observed in H520 cells from the respiratory system, BCP-1 and BJAB cells from the immune system, and primary human umbilical vein endothelial cells (HUVEC) from the reproductive system for SARS-CoV-2 but not SARS-CoV pseudoviruses. In contrast to SARS-CoV and SARS-CoV-2 pseudoviruses, all cell lines infected by VSV-G pseudovirus uniformly produced strong luciferase signals across all six cell lines examined (Figure 1B). These results indicated that SARS-CoV and SARS-CoV-2 pseudoviruses had tropism for specific types of cells.

3.2 | Entry-related recombinant proteins interfere with infection of SARS-CoV-2 and SARS-CoV pseudoviruses

Entry of SARS-CoV-2 into cells is mediated by the S protein through RBD interaction with cellular receptor(s).[13,14] To demonstrate the specificity of the pseudovirus infections, we performed blocking assays using S1 and RBD fusion recombinant proteins in Huh-7 cells, which had the highest pseudovirus infection levels (Figure 1A). Both S1 and RBD recombinant proteins effectively blocked the infection of SARS-CoV-2 pseudovirus in a dose-dependent manner, reducing luciferase signals by >60 to >95% at the highest dose of 25 μg/ml, respectively (Figure 2A,B). In contrast, a control hFc recombinant protein did not block any infectivity of both SARS-CoV-2 and SARS-CoV pseudoviruses (Figure S1). Recombinant ACE2 protein also effectively blocked the infection of SARS-CoV-2 in a dose-dependent manner, reducing infection by >95% at the highest dose of 25 μg/ml (Figure 2C). Interestingly, only marginal reduction of infectivity was observed when Kim-1 and NRP-1 recombinant proteins were used in the blocking assay. Although the inhibitory effects were statistically significant in one-way ANOVA analyses ($p = 0.0023$ for Kim-1 and $p = 0.0136$ for the NRP-1), no statistical difference was detected between individual blocking groups at any concentrations and the unblocked group (Figure 2D,E), suggesting weak roles of Kim-1 and NRP-1 proteins in SARS-CoV-2

FIGURE 2 Blocking of infection by SARS-CoV-2 and SARS-CoV pseudoviruses with S1, RBD, and other recombinant proteins of entry-related factors in Huh-7 cells. (A–E) Blocking of infection of SARS-CoV-2 and SARS-CoV pseudoviruses by S1 (A), RBD (B), ACE2 (C), Kim-1 (D), and NRP-1 (E) recombinant proteins. ANOVA analysis was performed if multiple samples were involved. *p*-value was calculated by unpaired two-tailed Student's *t* test between uninfected cells and untreated infected cells, and between treated group and untreated infected group. $p < 0.05$ was considered as statistically significant. ANOVA, analysis of variance; RBD, receptor-binding domain; Kim-1, kidney injury molecule-1; NRP-1, neuropilin-1; SARS-CoV-2, severe acute respiratory syndrome coronavirus 2; SARS-CoV, severe acute respiratory syndrome coronavirus

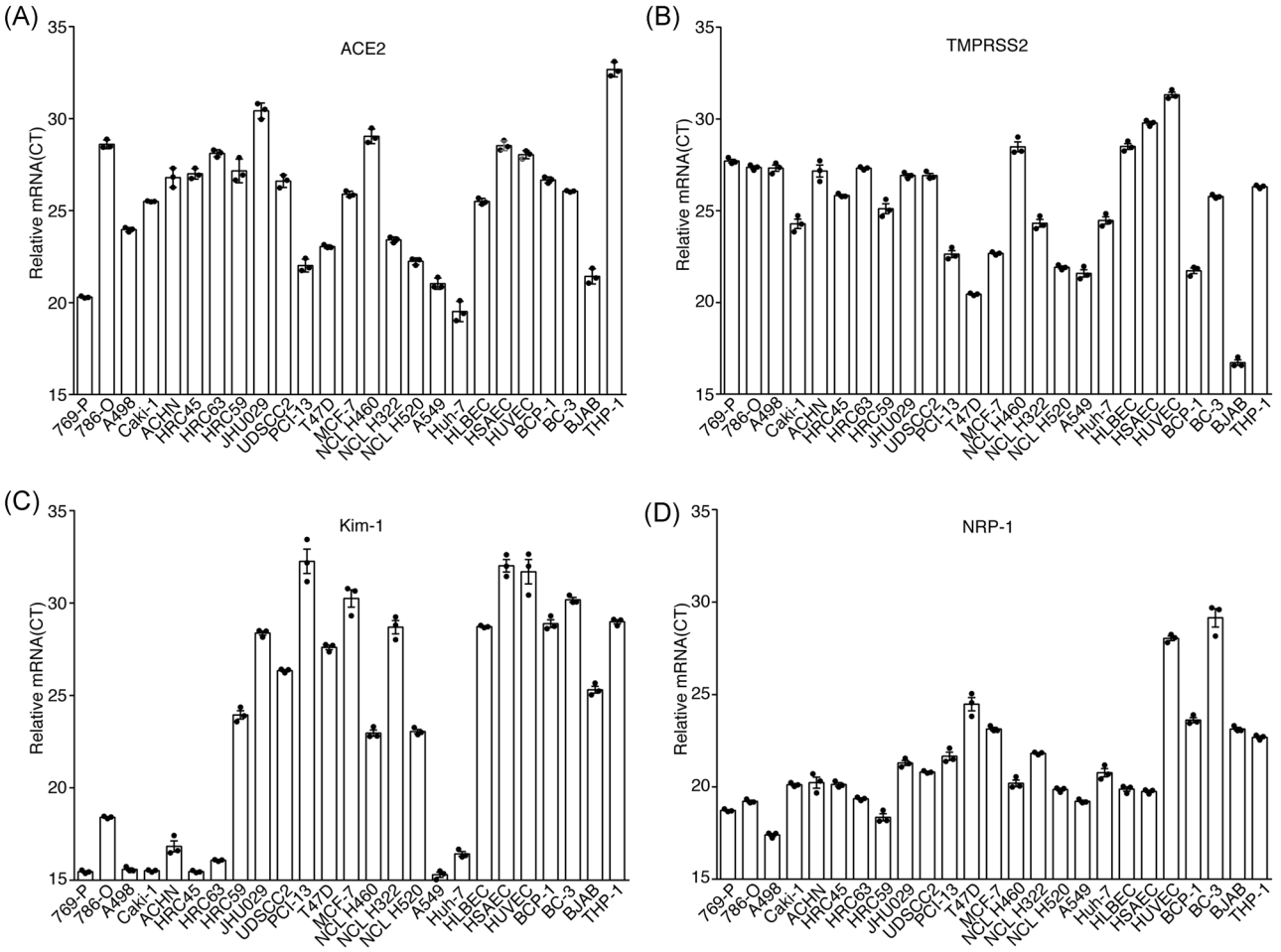

FIGURE 3 mRNA expression of ACE2, TMPRSS2, Kim-1, and NRP-1 in different types of cells from five human organ systems was analyzed by RT-qPCR. (A–D) Relative mRNA expression levels of ACE2 (A), TMPRSS2 (B), Kim-1 (C), and NRP-1 (D) presented as relative C_t values. β-actin gene was used for normalization. Kim-1, kidney injury molecule-1; mRNA, messenger RNA; NRP-1, neuropilin-1; RT-qPCR, real-time quantitative polymerase chain reaction; TMPRSS2, transmembrane serine protease 2

infection. Similar results were observed for SARS-CoV pseudovirus (Figure 2A–E).

3.3 | mRNA and protein expression levels of SARS-CoV-2 entry-related factors ACE2, TMPRSS2, Kim-1 and NRP-1

To examine cellular receptor abundance as contributing factors to pseudovirus infectivity (Figure 1A), we performed RT-qPCR to detect the mRNA levels of ACE2, TMPRSS2, Kim-1, and NRP-1 genes and presented the results as C_t values (Figure 3). There was no obvious correlation of SARS-CoV-2 pseudovirus infectivity with the mRNA levels of these cellular genes. Among cells with high SARS-CoV-2 pseudovirus infectivity, A549, 769-P, A498, and Huh-7 cells had relatively higher ACE2 expression levels (C_t values lower than 25) while JHU029, HLBEC, HSAEC, 786-O, and HRC45 cells had relatively lower ACE2 expression levels; and only A549 and Huh-7 cells had relatively higher TMPRSS2 expression levels (C_t values lower than 25) (Figure 3). Numerous cell lines had extremely high Kim-1 expression levels (C_t values lower than 18); however, among cells with high SARS-CoV-2 pseudovirus infectivity, A549, 769-P, A498, Huh-7, 786-O, and HRC45 cells had relatively higher Kim-1 expression levels (C_t values lower than 20) while JHU029, HLBEC, and HSAEC cells had relatively lower Kim-1 expression levels (Figure 3). Most of the cell lines and primary cells had robust NRP-1 expression levels (C_t values lower than 25 C_t) except HUVEC and BC-3 cells (Figure 3).

We then examined expression levels of ACE2, TMPRSS2, Kim-1, and NRP-1 proteins by Western blotting (Figure 4A). Despite some discrepancies, the protein levels were in general in agreement with the mRNA levels of genes encoding these proteins. For ACE2 protein, we detected two bands representing the glycosylated and unglycosylated forms (gly-ACE2 and ungly-ACE2) with the expected molecular mass sizes of ~85 kD and ~120 kD, respectively (Figure 4A).[31] Treatment of cell lysate with

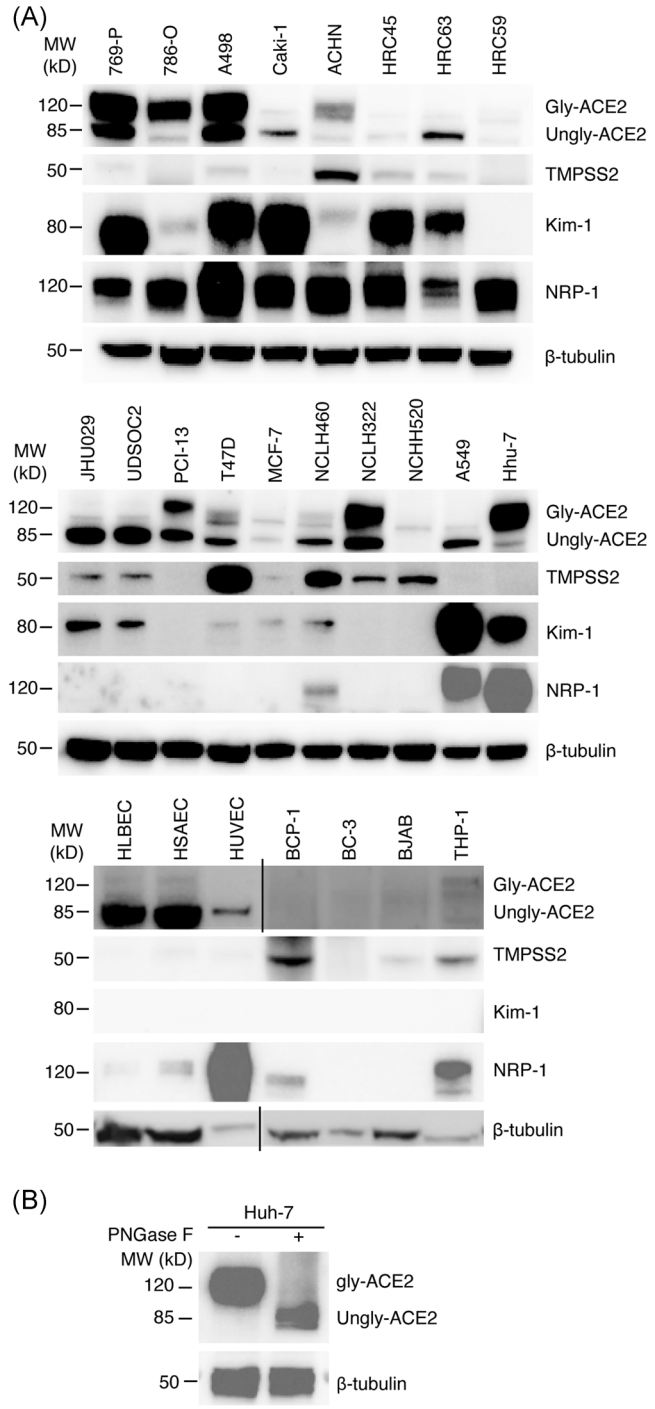

FIGURE 4 Expression levels of ACE2, TMPRSS2, Kim-1, and NRP-1 proteins in different cell lines/types, and examination of ACE glycosylation in Huh-7 cells analyzed by Western blot analysis. (A) Expression levels of ACE2, TMPRSS2, Kim-1, and NRP-1 proteins in different cell lines/types. Results showed that there are different expression profiles of ACE2, TMPRSS2, Kim-1, and NRP-1 in different cell lines/types. (B) Examination of ACE glycosylation in Huh-7 cells. Untreated and PNGase F-treated cell lysates were examined. β-tubulin was used for loading normalization. Two bands of ~85 kD and ~120 kD were detected for ACE2 protein representing the unglycosylated and glycosylated forms of ACE2 (ungly-ACE2 and gly-ACE2), respectively. Kim-1, kidney injury molecule-1; NRP-1, neuropilin-1; TMPRSS2, transmembrane serine protease 2

PNGase F, which removed the carbohydrate, indeed shifted all the gly-ACE2 to ungly-ACE2 in Huh-7 cells (Figure 4B). For cells that had high SARS-CoV-2 pseudovirus infectivity, 769-P, 786-O, A498, JHU029, HLBEC, HSAEC, and Huh-7 cells had overall relatively higher levels of ACE2 protein, of which 769-P, 786-O, A498, and Huh-7 cells had relatively higher levels of gly-ACE2, while A549 cells had a relatively low expression level and HRC45 cells had an almost undetectable level of ACE2 protein (Figure 4A). The expression levels of TMPSS2 protein were in general low in most of these cell lines and primary cells except T47D and H460 cells (Figure 4A). Among cells that had relatively higher levels of SARS-CoV-2 pseudovirus infectivity, 769-P, A498, HRC45, A549, and Huh-7 cells had relatively higher levels of Kim-1 protein, while 786-O, JHU029, HLBEC, and HSAEC cells had relatively lower or undetectable levels of Kim-1 protein (Figure 4A). For cells that had relatively higher levels of SARS-CoV-2 pseudovirus infectivity, relatively higher levels of NRP-1 protein were detected in 769-P, 786-O, A498, HRC45, A549, and Huh-7 cells while JHU029, HLBEC, and HSAEC cells had relatively lower or undetectable NRP-1 protein levels (Figure 4A). Overall, cells with high SARS-CoV-2 pseudovirus infectivity had relatively higher levels of ACE2 and gly-ACE2 proteins (769-P, 786-O, A498, JHU029, HLBEC, HSAEC, and Huh-7) or Kim-1 and NRP-1 proteins (A549 and HRC45).

We further examined the expression of ACE2, TMPRSS2, Kim-1, and NRP-1 proteins by IFA in selected types of cells including 769-P, HRC45, HLBEC, HSAEC, and Huh-7 cells with relatively higher levels of SARS-CoV-2 pseudovirus infectivity, and ACHN, MCF-7, H322, and H520 cells with relatively lower levels of SARS-CoV-2 pseudovirus infectivity (Figure 5). Overall, the staining intensities of all four proteins in different types of cells were consistent with their levels detected by Western blotting. No difference in the staining pattern of the four proteins in different types of cells was observed (Figure 5).

3.4 | Correlation of SARS-CoV-2 pseudovirus infectivity with expression levels of entry-related proteins

We examined the correlation between SARS-CoV-2 pseudovirus infectivity and expression levels of ACE2, TMPRSS2, Kim-1, and NRP-1 proteins (Figure 1A). SARS-CoV-2 pseudovirus infectivity had a positive correlation with the gly-ACE2 protein level, approaching statistical significance ($r = 0.3840$, $p = 0.0581$), but not with unglycosylated ACE2 ($r = 0.1651$, $p = 0.4303$) (Figure 6A,B). Similarly, SARS-CoV pseudovirus infectivity had a strong positive correlation with gly-ACE2 ($r = 0.6140$, $p = 0.0011$) but not ungly-ACE2 ($r = 0.03706$, $p = 0.8604$) (Figure 6C,D). These results confirmed the critical role of ACE2 in SARS-CoV-2 and SARS-CoV infection, and that glycosylation may be essential for entry, particularly for SARS-CoV. There was no correlation between SARS-CoV-2 pseudovirus infectivity and the expression of TMPRSS2 or

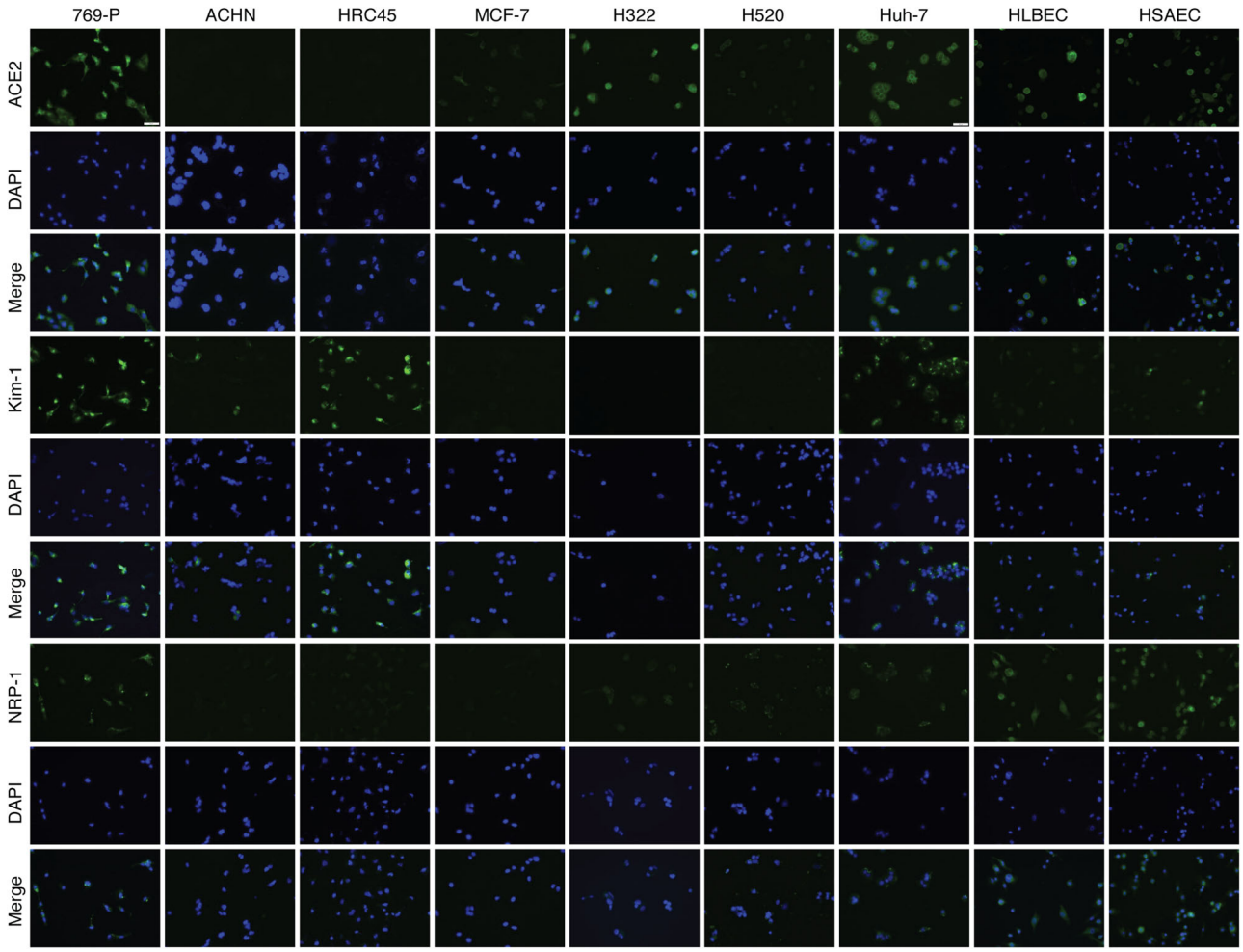

FIGURE 5 Expression levels and patterns of ACE2, Kim-1, and NRP-1 proteins in nine selected cell types/lines analyzed by IFA. IFA, Immunofluorescence assay; Kim-1, kidney injury molecule-1; NRP-1, neuropilin-1

Kim-1 protein (Figure 6E,G). However, there was a weak correlation between SARS-CoV-2 pseudovirus infectivity and the expression of NRP-1 protein approaching statistical significance ($r = 0.3455$, $p = 0.0907$) (Figure 6I). There was no correlation between SARS-CoV pseudovirus infectivity and the expression of TMPRSS2 or NRP-1 protein (Figure 6F,J). However, there was a correlation between SARS-CoV pseudovirus infectivity and the expression of Kim-1 protein, approaching statistical significance ($r = 0.3896$, $p = 0.0542$) (Figure 6H). Hence, in addition to gly-ACE2 protein, NRP-1 protein expression might be important for SARS-CoV-2 infection while Kim-1 expression might be important for SARS-CoV infection.

4 | DISCUSSION

Infection by SARS-CoV-2 has been detected in diverse types of cells and tissues such as AECs in alveoli, nasopharyngeal region, kidney, pneumocytes, alveolar macrophages, and lymph nodes, and so on.[4,32–35] We have recently examined lung tissues from patients with severe COVID-19 and found extensive expression of SARS-CoV-2 proteins in a wide range of parenchymal and immune cells.[10] Results of these studies suggest that SARS-CoV-2 could infect a wide range of cell types.

In the current study, we investigated the cell tropism of SARS-CoV-2 using a pseudovirus to infect 22 cell lines and 3 types of primary cells isolated from respiratory, urinary, immune, digestive, and reproductive systems (Figure 1A and Table 3). At least one cell line or one type of primary cell from each of five body systems was infected by SARS-CoV-2 pseudovirus. These results confirm the broad tropism of SARS-CoV-2, which likely contributes to the complex pathological syndromes in COVID-19 patients. Interestingly, broad infection by SARS-CoV pseudovirus in at least one cell line or cell type of these body systems except the immune system was also observed. It is known that SARS-CoV pathology is mostly localized to the respiratory system, and to a lesser extent with other organ systems. This could be due to its more rapid progression and higher case fatality rate than SARS-CoV-2 infection,[36] which might mask

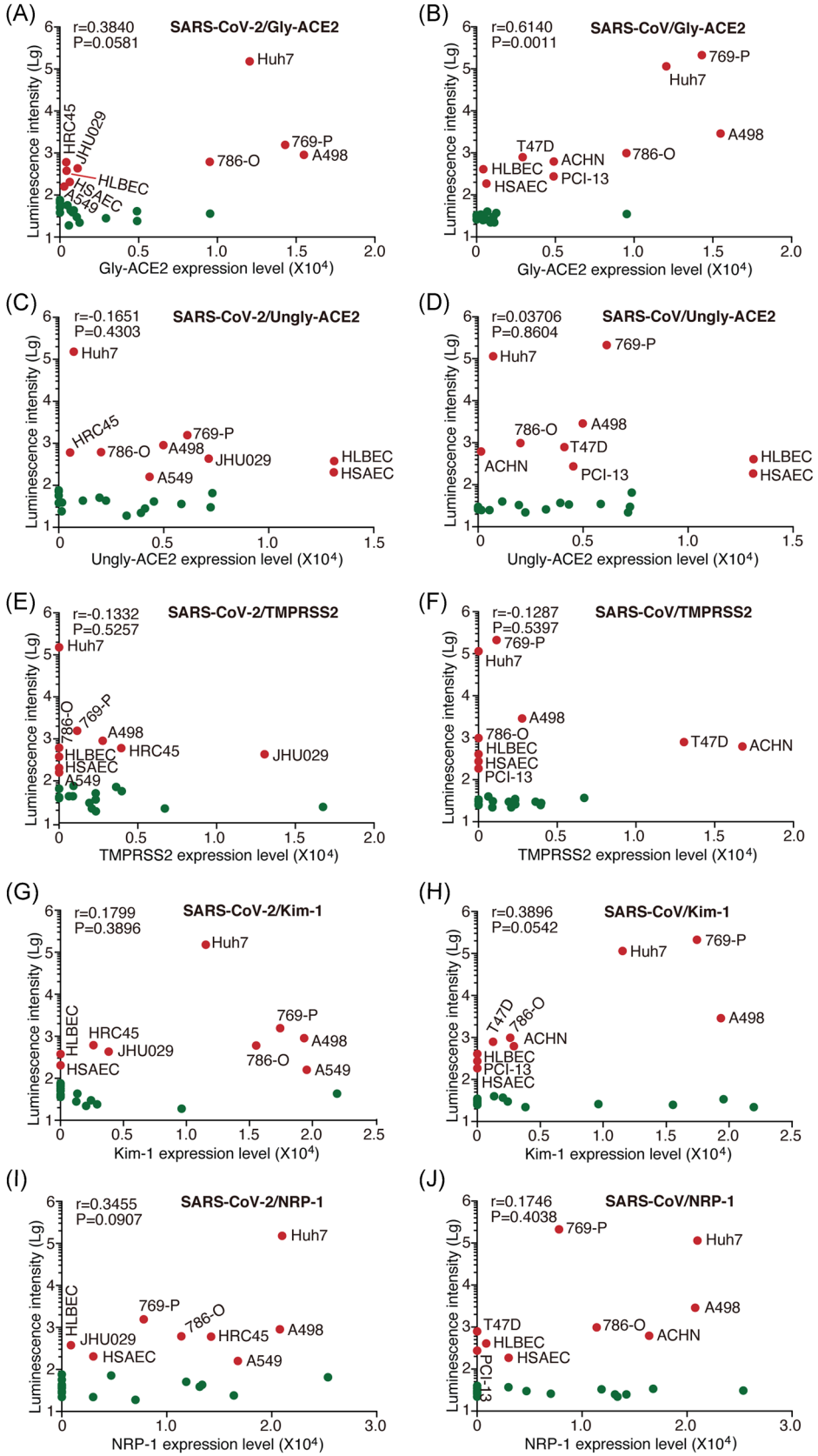

FIGURE 6 (See caption on next page)

nonrespiratory pathologies that would otherwise occur with SARS-CoV infection.

Close to half of the cell lines examined in this study were refractory to SARS-CoV-2 pseudovirus infection. It is possible that complex factors might be involved in regulating SARS-CoV-2 infection in vivo. Indeed, numerous cytokines including type 1 and 2 interferons have been shown to upregulate the expression of ACE2 and promote SARS-CoV-2 infection.[37,38] Further studies to identify factors that might contribute to SARS-CoV-2 infection and spread are warranted.

Entry of SARS-CoV-2 and SARS-CoV is primarily mediated by viral S1 protein through its interaction with cellular receptors.[39] Our results show an efficient inhibitory effect of S1 and RBD recombinant proteins on the infection of both SARS-CoV-2 and SARS-CoV pseudoviruses, and that RBD recombinant protein had a more potent inhibitory effect, confirming the essential role of S1 protein in mediating the infection of both SARS-CoV-2 and SARS-CoV through the RBD domain.

Numerous cellular proteins have been shown to have roles in SARS-CoV-2 cell entry including ACE2, TMPRSS2, Kim-1, and NRP-1 proteins.[11,24,40–42] RNAseq has demonstrated high ACE2 expression in diverse types of cells including pulmonary AT2, respiratory epithelial, myocardial, digestive tract epithelial, nasal goblet secretory and kidney cells, ileal absorptive enterocytes, and salivary glands.[37,43,44] IFA staining has revealed wide expression of ACE2 protein in different parenchymal and immune cell types.[10] ACE2 protein is present in a different part of the kidney and has a high expression level,[45,46] explaining why SARS-CoV-2 kidney infection had a significantly higher risk of in-hospital death.[47]

Although most of the SARS-CoV-2-infected cells are ACE2-positive in lung tissues from COVID-19 patients, we have also observed ACE2-negative SARS-CoV-2-infected cells, suggesting possible SARS-CoV-2 infection through an ACE2-independent mechanism.[10] Indeed, among the cell lines and primary cell types that were positively infected by SARS-CoV-2 pseudovirus, we also found that A549 and HRC45 cells had extremely weak levels of ACE2 protein expression (Figure 4A). Nevertheless, we found a trend of positive correlation of SARS-CoV-2 pseudovirus infectivity with the level of gly-ACE2 protein but not ungly-ACE2 protein (Figure 6A,B).

It has been reported that in engineered human tissue, SARS-CoV-2 infection was inhibited by soluble human ACE2.[48] Our results showed that recombinant ACE2 protein effectively blocked the infectivity of SARS-CoV-2 pseudovirus in Huh-7 cells and that the ACE2 inhibitory effect occurred in a lower concentration than that reported in a previous study[48] (Figure 2C). These results support an important role of ACE2 protein, particularly gly-ACE2 protein, in SARS-CoV-2 infection of ACE2-dependent cells. On the other hand, we found a statistically significant positive correlation of SARS-CoV pseudovirus infectivity with the levels of gly-ACE2 protein but not ungly-ACE2 protein. Hence, compared with SARS-CoV, SARS-CoV-2 infection is less dependent on gly-ACE2, which might explain its promiscuous broad tropism and more infectious nature.[10] In fact, the dual nature of human ACE2 glycosylation in binding to SARS-CoV-2 spike has been reported.[49] Specifically, the glycans at the N90 and N322 glycosylation sites had opposite effects on S protein binding.[49]

Interestingly, A549 and HRC45 cells had a robust SARS-CoV-2 pseudovirus infection but weak levels of ACE2 protein and both expressed strong levels of Kim-1 and NRP-1 proteins (Figure 4). We found a trend of positive correlation of SARS-CoV-2 pseudovirus infectivity with the level of NRP-1 protein. Furthermore, recombinant NRP-1 protein blocked SARS-CoV-2 pseudovirus in a dose-dependent fashion albeit no significant difference was detected when individual recombinant protein treated groups were compared with the untreated infected group. These results suggest that NRP-1 might mediate SARS-CoV-2 infection in ACE2-negative cells though this role is less obvious in ACE2-dependent SARS-CoV-2 infection. On the other hand, we did not find any correlation of SARS-CoV pseudovirus infectivity with the level of NRP-1 protein level. In contrast, the Kim-1 protein level was not correlated with SARS-CoV-2 pseudovirus infectivity, however, it was weakly correlated with the SARS-CoV pseudovirus infectivity. Similar to NRP-1, recombinant Kim-1 protein blocked infection of both SARS-CoV-2 and SARS-CoV pseudoviruses in a dose-dependent fashion in one-way ANOVA analysis albeit no significant difference was detected when the treated groups were compared with the untreated infected group. Hence, the roles of NRP-1 and Kim-1 proteins in infection of SARS-CoV-2 or SARS-CoV are likely minor, if any, in ACE2-dependent SARS-CoV-2 infection.

Taken together, SARS-CoV-2 can infect a wide range of cells from different human body systems. As factors that mediate SARS-CoV-2 infection, ACE2, TMPRSS2, Kim-1, and NRP-1 are broadly distributed in cells from different body systems. In cells that SARS-CoV-2 infection depends on ACE2 protein, TMPRSS2, Kim-1, and NRP-1 proteins are likely not critical for SARS-CoV-2 infection. However, in cells that SARS-CoV-2 infection does not depend on

FIGURE 6 Analyses of the correlation between the infectivity of SARS-CoV-2 or SARS-CoV and the protein expression levels of entry-related factors. (A–J) Correlation of the infectivity of SARS-CoV-2 (A, C, E, G, and I) or SARS-CoV (B, D, F, H, and J) with glycosylated ACE2 (gly-ACE2) (A and B), unglycosylated ACE2 (ungly-ACE2) (C and D), TMPRSS2 (E and F), Kim-1 (G and H) and NRP-1 (I and J). The "red" dots represent cell lines/types that were infected by the pseudoviruses. The "green" dots represent cell lines/types that were not infected by the pseudoviruses. Kim-1, kidney injury molecule-1; NRP-1, neuropilin-1; SARS-CoV-2, severe acute respiratory syndrome coronavirus 2; SARS-CoV, severe acute respiratory syndrome coronavirus; TMPRSS2, transmembrane serine protease 2

ACE2 proteins, Kim-1 and NRP-1 proteins are likely to mediate SARS-CoV-2 infection. The usage of these diverse factors in cell entry might endow the promiscuity of SARS-CoV-2 infection, and hence broad cell tropism.

ACKNOWLEDGMENTS

The authors thank Dr. Wei Cun at the Institute of Medical Biology, Chinese Academy of Medical Sciences & Peking Union Medical College, Beijing, China for providing us the plasmids for generating the pseudoviruses, and Dr. Siddharth Balachandran (Fox Chase Cancer Center) for providing the HRC59 cell line. The authors also thank all the Gao Lab members for their helpful discussions and technical support. This study was supported by UPMC Hillman Cancer Center Startup Fund and Pittsburgh Foundation Endowed Chair in Drug Development for Immunotherapy (to SJG). This study was in part supported by National Cancer Institute Award P30CA047904.

CONFLICT OF INTERESTS

The authors declare that there are no conflict of interests.

AUTHOR CONTRIBUTIONS

Conceptualization, plan, and management: Shou-Jiang Gao. *Experimental design*: Fei Zhang and Shou-Jiang Gao. *Execution of experiments, acquisition, analysis, or interpretation of data*: Fei Zhang, Wan Li, Jian Feng, Suzane Ramos da Silva, Enguo Ju, Hu Zhang, Yuan Chang, Patrick S. Moore, Haitao Guo and Shou-Jiang Gao. *Drafting and revision of the manuscript*: Fei Zhang and Shou-Jiang Gao. *Manuscript editing and approval*: Fei Zhang, Wan Li, Jian Feng, Suzane Ramos da Silva, Enguo Ju, Hu Zhang, Yuan Chang, Patrick S. Moore, Haitao Guo, and Shou-Jiang Gao.

DATA AVAILABILITY STATEMENT

The data that support the findings of this study are available from the corresponding author upon reasonable request.

ORCID

Suzane Ramos da Silva https://orcid.org/0000-0002-0768-8421
Enguo Ju https://orcid.org/0000-0003-0968-9994
Haitao Guo https://orcid.org/0000-0002-7146-916X
Shou-Jiang Gao https://orcid.org/0000-0001-6194-1742

REFERENCES

1. Harrison AG, Lin T, Wang P. Mechanisms of SARS-CoV-2 transmission and pathogenesis. *Trends Immunol*. 2020;41(12):1100-1115. https://doi.org/10.1016/j.it.2020.10.004
2. Hu B, Guo H, Zhou P, Shi ZL. Characteristics of SARS-CoV-2 and COVID-19. *Nat Rev Microbiol*. 2021;19(3):141-154. https://doi.org/10.1038/s41579-020-00459-7
3. Wang Y, Wang Y, Chen Y, Qin Q. Unique epidemiological and clinical features of the emerging 2019 novel coronavirus pneumonia (COVID-19) implicate special control measures. *J Med Virol*. 2020;92(6):568-576. https://doi.org/10.1002/jmv.25748
4. Su H, Yang M, Wan C, et al. Renal histopathological analysis of 26 postmortem findings of patients with COVID-19 in China. *Kidney Int*. 2020;98(1):219-227. https://doi.org/10.1016/j.kint.2020.04.003
5. Sun J, Zhu A, Li H, et al. Isolation of infectious SARS-CoV-2 from urine of a COVID-19 patient. *Emerg Microbes Infect*. 2020;9(1):991-993. https://doi.org/10.1080/22221751.2020.1760144
6. Wang Y, Liu S, Liu H, et al. SARS-CoV-2 infection of the liver directly contributes to hepatic impairment in patients with COVID-19. *J Hepatol*. 2020;73(4):807-816. https://doi.org/10.1016/j.jhep.2020.05.002
7. Mao Q, Chu S, Shapiro S, Bliss JM, De Paepe ME. Increased placental expression of angiotensin-converting enzyme 2, the receptor of SARS-CoV-2, associated with hypoxia in twin anemia-polycythemia sequence (TAPS). *Placenta*. 2021;105:7-13. https://doi.org/10.1016/j.placenta.2021.01.008
8. Zang R, Gomez Castro MF, McCune BT, et al. TMPRSS2 and TMPRSS4 promote SARS-CoV-2 infection of human small intestinal enterocytes. *Sci Immunol*. 2020;5(47), https://doi.org/10.1126/sciimmunol.abc3582
9. Wang C, Xie J, Zhao L, et al. Alveolar macrophage dysfunction and cytokine storm in the pathogenesis of two severe COVID-19 patients. *EBioMedicine*. 2020;57:102833. https://doi.org/10.1016/j.ebiom.2020.102833
10. Ramos da Silva S, Ju E, Meng W, et al. Broad SARS-CoV-2 cell tropism and immunopathology in lung tissues from fatal COVID-19. *J Infect Dis*. 2021;223:1842-1854. https://doi.org/10.1093/infdis/jiab195
11. Wahba L, Jain N, Fire AZ, et al. A pneumonia outbreak associated with a new coronavirus of probable bat origin. *Nature*. 2020;579(7798):270-273. https://doi.org/10.1038/s41586-020-2012-7
12. Harcourt J, Tamin A, Lu X, et al. Severe acute respiratory syndrome coronavirus 2 from patient with coronavirus disease, United States. *Emerg Infect Dis*. 2020;26(6):1266-1273. https://doi.org/10.3201/eid2606.200516
13. Lokugamage KG, Hage A, Schindewolf C, Rajsbaum R, Menachery VD. SARS-CoV-2 is sensitive to type I interferon pretreatment. *bioRxiv*. 2020. https://doi.org/10.1101/2020.03.07.982264
14. Hui KPY, Cheung M-C, Perera RAPM, et al. Tropism, replication competence, and innate immune responses of the coronavirus SARS-CoV-2 in human respiratory tract and conjunctiva: an analysis in ex-vivo and in-vitro cultures. *Lancet Respir Med*. 2020;8(7):687-695. https://doi.org/10.1016/s2213-2600(20)30193-4
15. Shuai H, Chu H, Hou Y, et al. Differential immune activation profile of SARS-CoV-2 and SARS-CoV infection in human lung and intestinal cells: implications for treatment with IFN-β and IFN inducer. *J Infect*. 2020;81(4):e1-e10. https://doi.org/10.1016/j.jinf.2020.07.016
16. Felgenhauer U, Schoen A, Gad HH, et al. Inhibition of SARS-CoV-2 by type I and type III interferons. *J Biol Chem*. 2020;295(41):13958-13964. https://doi.org/10.1074/jbc.AC120.013788
17. Chu H, Chan JF, Yuen TT, et al. Comparative tropism, replication kinetics, and cell damage profiling of SARS-CoV-2 and SARS-CoV with implications for clinical manifestations, transmissibility, and laboratory studies of COVID-19: an observational study. *Lancet Microbe*. 2020;1(1):e14-e23. https://doi.org/10.1016/s2666-5247(20)30004-5
18. Harcourt J, Tamin A, Lu X, et al. Isolation and characterization of SARS-CoV-2 from the first US COVID-19 patient. *bioRxiv*. 2020. https://doi.org/10.1101/2020.03.02.972935
19. Li W, Moore MJ, Vasilieva N, Sui J. Angiotensin-converting enzyme 2 is a functional receptor for the SARS coronavirus. *Nature*. 2003;426:450-454.
20. Wei J, Alfajaro MM, DeWeirdt PC, et al. Genome-wide CRISPR screens reveal host factors critical for SARS-CoV-2 infection. *Cell*. 2021;184(1):76-91. e13. https://doi.org/10.1016/j.cell.2020.10.028

21. Stopsack KH, Mucci LA, Antonarakis ES, Nelson PS, Kantoff PW. TMPRSS2 and COVID-19: serendipity or opportunity for intervention? *Cancer Discov*. 2020;10(6):779-782. https://doi.org/10.1158/2159-8290.CD-20-0451
22. Ichimura T, Mori Y, Aschauer P, et al. KIM-1/TIM-1 is a receptor for SARS-CoV-2 in lung and kidney. *medRxiv*. 2020. https://doi.org/10.1101/2020.09.16.20190694
23. Han WK, Bailly V, Abichandani R, Thadhani R, Bonventre JV. Kidney injury molecule-1 (KIM-1): a novel biomarker for human renal proximal tubule injury. *Kidney Int*. 2002;62(1):237-244. https://doi.org/10.1046/j.1523-1755.2002.00433.x
24. Cantuti-Castelvetri L, Ojha R, Pedro LD, et al. Neuropilin-1 facilitates SARS-CoV-2 cell entry and infectivity. *Science*. 2020;370:856-860.
25. Kielian M. Enhancing host cell infection by SARS-CoV-2. *Science*. 2020;370(6518):765-766.
26. Qi F, Qian S, Zhang S, Zhang Z. Single cell RNA sequencing of 13 human tissues identify cell types and receptors of human coronaviruses. *Biochem Biophys Res Commun*. 2020;526(1):135-140. https://doi.org/10.1016/j.bbrc.2020.03.044
27. Hikmet F, Mear L, Edvinsson A, Micke P, Uhlen M, Lindskog C. The protein expression profile of ACE2 in human tissues. *Mol Syst Biol*. 2020;16(7):e9610. https://doi.org/10.15252/msb.20209610
28. Sungnak W, Huang N, Bécavin C, et al. SARS-CoV-2 entry factors are highly expressed in nasal epithelial cells together with innate immune genes. *Nat Med*. 2020;26(5):681-687. https://doi.org/10.1038/s41591-020-0868-6
29. Lukassen S, Chua RL, Trefzer T, et al. SARS-CoV-2 receptor ACE2 and TMPRSS2 are primarily expressed in bronchial transient secretory cells. *EMBO J*. 2020;39(10):e105114. https://doi.org/10.15252/embj.20105114
30. Pu T, Ding C, Li Y, et al. Evaluate severe acute respiratory syndrome coronavirus 2 infectivity by pseudoviral particles. *J Med Virol*. 2020;92(9):1609-1614. https://doi.org/10.1002/jmv.25865
31. Jia HP, Look DC, Tan P, et al. Ectodomain shedding of angiotensin converting enzyme 2 in human airway epithelia. *Am J Physiol Lung Cell Mol Physiol*. 2009;297:L84-L96. https://doi.org/10.1152/ajplung.00071.2009.-Angiotensin-converting
32. Sauter JL, Baine MK, Butnor KJ, et al. Insights into pathogenesis of fatal COVID-19 pneumonia from histopathology with immunohistochemical and viral RNA studies. *Histopathology*. 2020;77(6):915-925. https://doi.org/10.1111/his.14201
33. Pesaresi M, Pirani F, Tagliabracci A, et al. SARS-CoV-2 identification in lungs, heart and kidney specimens by transmission and scanning electron microscopy. *Eur Rev Med Pharmacol Sci*. 2020;24:24-5188.
34. Parada D, Peña KB, Gumà J, Guilarte C, Riu F. Liquid-based cytological and immunohistochemical study of nasopharyngeal swab from persons under investigation for SARS-CoV-2 infection. *Histopathology*. 2021;78(4):586-592. https://doi.org/10.1111/his.14257
35. Martines RB, Ritter JM, Matkovic E, et al. Pathology and pathogenesis of SARS-CoV-2 associated with fatal coronavirus disease, United States. *Emerg Infect Dis*. 2020;26(9):2005-2015. https://doi.org/10.3201/eid2609.202095
36. Nicholls J, Dong XP, Jiang G, Peiris M. SARS: clinical virology and pathogenesis. *Respirology*. 2003;8 Suppl(Suppl 1):S6-S8. https://doi.org/10.1046/j.1440-1843.2003.00517.x
37. Ziegler CGK, Allon SJ, Nyquist SK, et al. SARS-CoV-2 receptor ACE2 is an interferon-stimulated gene in human airway epithelial cells and is detected in specific cell subsets across tissues. *Cell*. 2020;181(5):1016-1035. https://doi.org/10.1016/j.cell.2020.04.035. e1019.
38. Zhuang MW, Cheng Y, Zhang J, et al. Increasing host cellular receptor-angiotensin-converting enzyme 2 expression by coronavirus may facilitate 2019-nCoV (or SARS-CoV-2) infection. *J Med Virol*. 2020;92(11):2693-2701. https://doi.org/10.1002/jmv.26139
39. Gordon DE, Jang GM, Bouhaddou M, et al. A SARS-CoV-2 protein interaction map reveals targets for drug repurposing. *Nature*. 2020;583(7816):459-468. https://doi.org/10.1038/s41586-020-2286-9
40. Yang C, Zhang Y, Zeng X, et al. Kidney injury molecule-1 is a potential receptor for SARS-CoV-2. *J Mol Cell Biol*. 2021;13:185-196. https://doi.org/10.1093/jmcb/mjab003
41. Hoffmann M, Kleine-Weber H, Schroeder S, et al. SARS-CoV-2 cell entry depends on ACE2 and TMPRSS2 and is blocked by a clinically proven protease inhibitor. *Cell*. 2020;181(2):271-280. https://doi.org/10.1016/j.cell.2020.02.052. e278.
42. Heurich A, Hofmann-Winkler H, Gierer S, Liepold T, Jahn O, Pohlmann S. TMPRSS2 and ADAM17 cleave ACE2 differentially and only proteolysis by TMPRSS2 augments entry driven by the severe acute respiratory syndrome coronavirus spike protein. *J Virol*. 2014;88(2):1293-1307. https://doi.org/10.1128/JVI.02202-13
43. Zou X, Chen K, Zou J, Han P, Hao J, Han Z. Single-cell RNA-seq data analysis on the receptor ACE2 expression reveals the potential risk of different human organs vulnerable to 2019-nCoV infection. *Front Med*. 2020;14(2):185-192. https://doi.org/10.1007/s11684-020-0754-0
44. Song J, Li Y, Huang X, et al. Systematic analysis of ACE2 and TMPRSS2 expression in salivary glands reveals underlying transmission mechanism caused by SARS-CoV-2. *J Med Virol*. 2020;92(11):2556-2566. https://doi.org/10.1002/jmv.26045
45. Cheng H, Wang Y, Wang GQ. Organ-protective effect of angiotensin-converting enzyme 2 and its effect on the prognosis of COVID-19. *J Med Virol*. 2020;92(7):726-730. https://doi.org/10.1002/jmv.25785
46. Hamming I, Timens W, Bulthuis ML, Lely AT, Navis G, van Goor H. Tissue distribution of ACE2 protein, the functional receptor for SARS coronavirus. A first step in understanding SARS pathogenesis. *J Pathol*. 2004;203(2):631-637. https://doi.org/10.1002/path.1570
47. Yang X, Yu Y, Xu J, et al. Clinical course and outcomes of critically ill patients with SARS-CoV-2 pneumonia in Wuhan, China: a single-centered, retrospective, observational study. *Lancet Respir Med*. 2020;8(5):475-481. https://doi.org/10.1016/s2213-2600(20)30079-5
48. Monteil V, Kwon H, Prado P, et al. Inhibition of SARS-CoV-2 infections in engineered human tissues using clinical-grade soluble human ACE2. *Cell*. 2020;181(4):905-913. https://doi.org/10.1016/j.cell.2020.04.004. e907.
49. Mehdipoura AR, Hummer G. Dual nature of human ACE2 glycosylation in binding to SARS-CoV-2 spike. *PNAS*. 2021;118(19), https://doi.org/10.1073/pnas.2100425118/-/DCSupplemental

SUPPORTING INFORMATION

Additional Supporting Information may be found online in the supporting information tab for this article.

How to cite this article: Zhang F, Li W, Feng J, et al. SARS-CoV-2 pseudovirus infectivity and expression of viral entry-related factors ACE2, TMPRSS2, Kim-1, and NRP-1 in human cells from the respiratory, urinary, digestive, reproductive, and immune systems. *J Med Virol*. 2021;93:6671-6685. https://doi.org/10.1002/jmv.27244